Published 2010 in Earth and Planetary Science Letters 297: 332-338 (http://dx.doi.org/10.1016/j.epsl.2010.06.035)

Salinity changes in the North West Pacific Ocean during the late Pliocene/early Quaternary from 2.73 Ma to 2.52 Ma

George E.A. Swann[a]*

[a]NERC Isotope Geosciences Laboratory, British Geological Survey, Keyworth, Nottingham, NG12 5GG, UK

* corresponding author gean@bgs.ac.uk

Abstract

Recent research has increasingly advocated a role for the North Pacific Ocean in modulating global climatic changes over both the last glacial cycle and further back into the geological record. Here a diatom $\delta^{18}O$ record is presented from Ocean Drilling Program Site 882 over the Pliocene/Quaternary boundary from 2.73 Ma to 2.52 Ma (MIS G6-MIS 99). Large changes in $\delta^{18}O_{diatom}$ of c. 4‰ from 2.73 Ma onwards are documented to occur on a timeframe broadly coinciding with glacial-interglacial cycles. These changes are primarily attributed to large scale inputs of meltwater from glacials surrounding the North Pacific Basin and the Bering Sea. Despite these inputs and associated change in surface water salinity, on the basis of existing opal and U^{k}_{37} temperature data and new modelled water column densities, no evidence exists to suggests a removal of the halocline stratification or a resumption of the high productivity system similar to that which prevailed prior to 2.73 Ma. The permanence of the halocline suggests that the region played a key role in driving global climatic changes over the early glacial-interglacial cycles that followed the onset of major Northern Hemisphere Glaciation by inhibiting deep water upwelling and ventilation of CO_2 to the atmosphere.

Keywords: Ocean Drilling Program, Leg 145, Site 882, diatom, isotope, halocline, meltwater, stratification

1 Introduction

In comparison to other sectors of the marine system such as the North Atlantic and Southern Oceans, the palaeoceanographic history of the North Pacific Ocean remains under-investigated. Research over the past decade has increasingly indicated that changes in the subarctic North West Pacific Ocean were critical in driving the global climate system from the warm, stable, conditions that prevailed during the early/mid Pliocene to the glacial-interglacial cycles that characterise the late Pliocene/Quaternary era (Haug et al., 1999, 2005; Sigman et al., 2004; Swann et al., 2006; Reynolds et al., 2008). These changes are marked by the influx of large volumes of freshwater at the onset of major Northern Hemisphere Glaciation (NHG) at 2.73 Ma, culminating in the transition from a mixed to a halocline, stratified, water column. With deep water

Published 2010 in Earth and Planetary Science Letters 297: 332-338 (http://dx.doi.org/10.1016/j.epsl.2010.06.035)

in the region rich in CO_2, the shift from an unstratified (upwelling) to stratified (no/minimal deep water upwelling) state has been associated with a significant reduction in surface water concentrations of CO_2 (pCO_2), reducing oceanic ventilation of CO_2 to the atmosphere and further permitting glacial advancement across the Northern Hemisphere (Haug et al., 1999).

In spite of the considerable palaeoceanographic research that has been undertaken in understanding the changes from a unstratified to stratified water column at 2.73 Ma, comparatively little research has been carried out to investigate further water column re-organizations during the glacial-interglacial cycles which follow this interval during the late Piacenzian (3.60-2.59 Ma) and Gelasian (2.59-1.81 Ma). In part this can be attributed to the the absence of sufficient numbers of foraminifera and other carbonate fossils in the sediment record for isotope/geochemical analyses. Furthermore, low opal MAR and other record of productivity have been interpreted to indicate that a stratified water column prevailed largely, but not completely, without interruption from 2.73 Ma through to the modern day (Haug et al., 1999; Sigman et al., 2004; Gebhardt et al., 2008). However, low resolution variations in diatom $\delta^{18}O$ ($\delta^{18}O_{diatom}$) and U^{k}_{37} Sea Surface Temperature (SST) of c. 5.0‰ and 9°C respectively from 2.73-2.61 Ma (Marine Isotope Stage (MIS) G6 to MIS 104) suggest that the region may have experienced marked changes in the post-2.73 Ma interval similar to those that occurred during the initial development of the halocline at 2.73 Ma (Haug et al., 2005; Swann et al., 2006).

At present the origin, temporal variability and implication for these changes remain unknown, particularly with regards to their impact on the strength of the regional halocline. Any weakening/strengthening of the halocline would be significant in altering the flux of nutrients and CO_2 rich deep water into the photic zone. Depending on the response of the biological pump, such changes could have altered the regional flux of CO_2 between the oceans/atmosphere (c.f. Gebhardt *et al.*, 2008) and so altered the global carbon budget and climatic changes over the Pliocene/Quaternary boundary. Here, in order to better understand the palaeoceanography of the subarctic North West Pacific Ocean, existing $\delta^{18}O_{diatom}$ records are extended and increased in resolution for the interval from 2.73 Ma to 2.52 Ma (MIS G6-MIS 99) at Ocean Drilling Program (ODP) Site 882.

2 Methods

Sediment samples from ODP Site 882 (Fig. 1) were prepared for diatom isotope analysis using techniques previously employed at this site (Swann et al., 2006; 2008). Samples were treated with 30% H_2O_2 and 5% HCl to remove organic material and carbonates respectively before being repeatedly mixed with sodium polytungstate at a series of specific gravities from 2.10 g/ml to 2.25 g/ml prior to a final sieving with a 5 μm cellulose nitrate membrane filter to remove all non-diatom contaminants. Previous research has demonstrated a possible size/species vital effect in $\delta^{18}O_{diatom}$ (Swann et al., 2007, 2008). Here such issues are circumvented by sieving and retaining solely the 75-150 µm size fraction for isotope analysis which is dominated by only two taxa (see Section 3). Sample purity was assessed through a combination of both light microscopy and Scanning Light Microscopy (SEM) with contaminated samples either re-cleaned or disregarded for isotope analysis. For light microscopy, sub-samples of the purified diatoms were mounted on a coverslip using a Naphrax® mounting media and checked for contamination on a 100 µm x 100 µm grid graticule following the semi-quantitative method of Morley et al., (2004). Diatom biovolumes were simultaneously assessed for each sample following the recommendations of Hillebrand et al., (1999) to determine the species origin of the isotope signal (see Swann et al., 2008 for further details). SEM analysis to verify sample purity and the reliability of the light microscopy observations were completed on randomly selected samples. Ages were calculated using a linear interpolation of sedimentation rates between tie-points derived from the astronomical calibrated of high resolution GRAPE density and magnetic susceptibility measurements (Tiedemann and Haug, 1995).

$\delta^{18}O_{diatom}$ was analysed using the step-wise fluorination methodology described in Leng and Sloane (2008). In brief, $\delta^{18}O_{diatom}$ was analysed with diatom -Si-OH layers stripped during a pre-fluorination outgassing stage in nickel reaction tubes using a BrF_5 regent at 250ºC for six minutes. Remaining oxygen from the -Si-O-Si layer was subsequently dissociated overnight using an excess of reagent at 550ºC with oxygen subsequently converted to CO_2 following the methodology of Clayton and Mayeda (1963). Following extraction, CO_2 was analysed for $\delta^{18}O$ using a Finnegan MAT 253 with values converted to the SMOW scale using a within-run laboratory diatom standard (BFC_{mod}) calibrated against NBS28. Analytical reproducibility for $\delta^{18}O_{diatom}$ was 0.3‰ (1σ).

3 Results

SEM and light microscopy observations indicate the lack of contamination within the analysed samples with sample purity constantly above 94% and typically between 98% and 100% (see Swann et al., 2006). Samples are dominated by two taxa, *Coscinodiscus marginatus* (Ehrenb.) and *Coscinodiscus radiatus* (Ehrenb.), the relative biovolumes of which vary throughout the core (Fig. 2). No correlation or relationships exists between $\delta^{18}O_{diatom}$ and *C. marginatus*/*C. radiatus* from 2.73 Ma to 2.52 Ma (r = -0.06/0.07), indicating the absence of species disequilibrium/isotope vital effects.

Measurements of $\delta^{18}O_{diatom}$ can be interpreted in the same way as $\delta^{18}O$ measurements of planktonic foraminifera ($\delta^{18}O_{foram}$) (Swann and Leng, 2009). Accordingly, variations in $\delta^{18}O_{diatom}$ reflect changes in global ice volume, SST and/or changes in the $\delta^{18}O$ composition of the ambient water within the photic zone ($\delta^{18}O_{water}$). Following the development of the halocline stratification system at 2.73 Ma, marked by a decrease in $\delta^{18}O_{diatom}$ of 4.6‰ (Swann et al., 2006), values of $\delta^{18}O_{diatom}$ remain low at c. 39-40‰ before subsequently rising to 43.4‰ at 2.69 Ma (Fig. 3). Following this transition at MIS G6, cyclic changes are apparent in $\delta^{18}O_{diatom}$ that are broadly in line with changes in glacial-interglacial conditions as monitored by a global stacked benthic $\delta^{18}O_{foram}$ record (Lisiecki and Raymo, 2005). This is marked by $\delta^{18}O_{diatom}$ values of ≥42.0‰ during interglacials, similar to conditions prior to 2.73 Ma in a mixed water column, with lower values prevalent during glacials. Of note are the relatively low opal MAR and prevalence of warm, c. 15-18°C U^{k}_{37} SST through these transitions until MIS 103 when peak SST decrease below 10°C before rising again to 13-15°C for MIS 102-99 (Haug et al., 2005) (Fig. 3).

Superimposed on these long-term changes in $\delta^{18}O_{diatom}$ are a series of short-lived fluctuations of c. 1-2‰. This is most apparent during MIS G1 and MIS 103 and indicate that the region was characterised by significant environmental changes over relatively short timeframes. The exception to this glacial-interglacial pattern occurs during MIS G5 and MIS 101-100. For MIS G5 the failure for $\delta^{18}O_{diatom}$ to increase above glacial values of c. 40.0‰ may simply reflect the extremely low resolution isotope record through this interval as well as the low magnitude nature of interglacial relative to other glacial-interglacial changes. However with the shift to higher $\delta^{18}O_{diatom}$ values during MIS 101 occurring during the second half of the interglacial at 2.56 Ma and continuing through the beginning of MIS 100, any link between $\delta^{18}O_{diatom}$ and glacial-interglacial cycles are tentative until investigation are conducted over longer time-frames and/or at other sites.

4 Discussion

The nature of the water column prior to 2.73 Ma, the transition to a halocline water column at this interval and the divergent trends in the $\delta^{18}O_{diatom}$ and planktonic $\delta^{18}O_{foram}$ records have previously been described (Haug et al., 1999; 2005; Sigman et al., 2004; Swann et al., 2006; Reynolds et al., 2008). The discussion below is therefore restricted to examining the changes in $\delta^{18}O_{diatom}$ following the 4.6‰ decrease in $\delta^{18}O_{diatom}$ and development of the regional halocline at 2.73 Ma.

4.1 Freshwater inputs

In the absence of a high resolution $\delta^{18}O_{diatom}$ record, it is not possible to investigate leads/lags between changes in $\delta^{18}O_{diatom}$ and benthic $\delta^{18}O_{foram}$/glacial-interglacial state. However the cyclic nature of the $\delta^{18}O_{diatom}$ record from 2.73 Ma onwards that broadly occurs over glacial-interglacial cycles, combined with the large isotope changes of up to 6‰, suggest that the region experienced large scale palaeoceanographic changes during the late Pliocene/early Quaternary era. Typical glacial-interglacial change in SST over this interval, ranging up to c. 3°C, can only account for c. 0.6‰ of the change in $\delta^{18}O_{diatom}$ when using a diatom-temperature coefficients of 0.2 ‰/°C (Brandriss et al., 1998; Moschen et al., 2005). Similarly, whole ocean changes in $\delta^{18}O$ due to variations in global ice volume are on the order of 0.8‰ (Lisiecki and Raymo, 2005). As such the large fluctuations in $\delta^{18}O_{diatom}$ of up to 6‰ over glacial-interglacial cycles must predominantly reflect a change in surface water $\delta^{18}O_{water}$, which can be calculated from $\delta^{18}O_{diatom}$ using a global stacked benthic $\delta^{18}O_{foram}$ record (Lisiecki and Raymo, 2005) and accounting for changes in SST using a U^{k}_{37} SST record from ODP Site 882 (Haug et al., 2005) and a diatom-temperature coefficient of 0.2‰/ºC (Brandriss et al., 1998; Moschen et al., 2005) (Fig. 4a). Whilst the initial decrease in $\delta^{18}O_{diatom}$ and shift to a halocline system at c. 2.73 may have been linked to the closure of the Panama Ocean gateway and an associated reduction in the Pacific Ocean deep water thermohaline circulation (Motoi et al., 2005), such a mechanism is not applicable to explain subsequent changes in $\delta^{18}O_{diatom}$ after this interval. Similarly, increases/decreases in the influx of water from regions south of ODP Site 882 are unlikely to explain the large changes in $\delta^{18}O_{water}/\delta^{18}O_{diatom}$ given that North West Pacific Ocean waters differ from the mid-latitude and tropical Pacific by only c. 1‰ (LeGrande and Schmidt, 2006). Although the expansion of sea-ice in the Bering Sea over the onset of major NHG may lead to variations in the $\delta^{18}O$ of water flowing from the north into the subarctic North West Pacific Ocean (IODP Expedition 323, Scientists, 2010), such variations are likely to be low given fractionation factors of 1.0026–1.0035 (Majoube, 1971; Lehmann and Siegenthaler, 1991; Macdonald et al., 1995). Accordingly, two processes exist to explain the large changes in $\delta^{18}O_{water}$ and $\delta^{18}O_{diatom}$. First are changes in Asian summer monsoon which may deliver freshwater both through direct changes in regional precipitation and/or via increased continental riverine inputs to the marine system via the Kuroshio current. Such a process has previously been proposed to have driven the transition from a mixed to stratified water column between 2.83-2.75 Ma (Nie et al., 2008). Second are increases in glacial meltwater to the region, which will be significantly enriched in ^{16}O relative to ^{18}O.

Records of SSS at ODP Site 1143 in the South China Sea suggest a progressive decrease in SSS from 2.73 Ma to 2.50 Ma in response to increased monsoonal precipitation and fluvial inputs (Tian et al., 2004, 2006). However these local salinity changes, accounting for a c. 1‰ fluctuation in $\delta^{18}O_{water}$ over glacial-interglacial cycles, from an area strongly influenced by the East Asian monsoon are considerable smaller than those observed here at the more remote, open ocean, ODP Site 882. Consequently, it is difficult to envisage how sufficient fluvial quantities of monsoonal freshwater could have been delivered to ODP Site 882 to explain the changes in $\delta^{18}O_{diatom}$. The relative importance of monsoonal activity can be further assessed using records of accumulation and magnetic susceptibility at the Chinese Loess Plateau in addition to Hm/Gt ratios from ODP Site 1143 in the South China Sea as a proxy for Asian monsoon precipitation (Sun and An, 2005; Sun et al., 2006; Zhang et al., 2009) (Fig, 2). Again, no significant relationship can be observed between these records and changes in $\delta^{18}O_{diatom}$ at ODP Site 882. Although lower $\delta^{18}O_{diatom}$ values from MIS G6-G4 coincide with increased monsoon activity and vice-versa during MIS G3, changes subsequent to this fail to follow a similar pattern with intervals of higher/lower $\delta^{18}O_{diatom}$ occurring during periods of both high and low, as well as increasing and decreasing, monsoon activity. Accordingly, although changes in monsoon activity can not be completely eliminated, based on the absence of any clear relationship and problems with delivering sufficient quantities of monsoonal freshwater to ODP Site 882, it is likely that its role in instigating the observed $\delta^{18}O_{diatom}$ variations be minimal compared to other mechanisms.

Instead, it is proposed that decreases/increases in $\delta^{18}O_{diatom}$ are primarily driven by increases/decreases in glacial meltwater input to the North Pacific Ocean over glacials/interglacials, as well as within the short term fluctuations in $\delta^{18}O_{diatom}$ for individual marine isotope stages. Whilst speculative, an advantage of such a mechanisms is that comparatively less water is needed to drive the observed changes in $\delta^{18}O_{diatom}$ than monsoonal inputs due to the significantly more negative $\delta^{18}O$ value of glacial sourced meltwater. Evidence from the North Atlantic Ocean showing that the $\delta^{18}O$ of glacial ice in the Pliocene was lower than the late Pleistocene provides a further means of potentially explaining the marked decrease in $\delta^{18}O_{diatom}$ during glacials (Bailey et al., 2010). Numerous sites may be acting as the source for any glacial meltwater to the region including the Bering Sea Basin, the Okhotsk and Kamchatka regions of Siberia as well as possible inputs from the Aleutian Islands and Southern Alaska (e.g., Kotilainen and Shackleton, 1995; McKelvey et al., 1995; St John and Krissek, 1999; Bigg et al., 2008). Due to the unknown isotopic composition of these ice-sheets and without knowing the relative contributions of meltwater from each locality, it is not possible to accurately calculate the salinity:$\delta^{18}O$ relationship for meltwater entering the region and so quantify actual changes in salinity. The range of possible Sea Surface Salinity (SSS) variability can, however, be estimated by using two extreme SSS:$\delta^{18}O$ ratio end-members of 1 and 0.5. Such end-member calculations, which assumes that the end-member relationship remains constant either at 1 or 0.5 throughout the analysed interval, indicates that SSS may have varied by up to 8 psu over the analysed interval with typical glacial-interglacial changes of 2-4 psu (Fig. 4b). These changes are comparable to SSS fluctuation of up to 4 psu in the North Atlantic Ocean during Heinrich events (Duplessy et al. 1993; Maslin et al., 1995; Seidov and Maslin, 1999), suggesting that similar magnitude meltwater events/ice surges may have marked the North Pacific Ocean over this interval.

On the one hand is it hard to envisage that ice-sheets around the North Pacific Basin would have been sufficiently developed during the late Pliocene to instigate a Heinrich equivalent event at ODP Site 882 given its open ocean position south of the sea-ice extent. However, strong evidence exists of increased IRD deposition at ODP Site 882 from 2.73 Ma, with changes broadly occurring in line with glacial-interglacial cycles and fluctuations in $\delta^{18}O_{diatom}$, suggests that regional ice-sheets were significantly developed over this interval (Krissek, 1995; Maslin et al., 1996; Haug et al., 1999) (Fig. 3). Evidence from the North Atlantic Ocean has also suggested a possible low threshold for ice-surging events in the Pliocene (Bailey et al., 2010). One scenario is that an initial strengthening of the water column stratification occurs at the beginning of each glacial/SSS decrease following an initial meltwater surge or reduced deep water exchanges. With subsequent meltwater inputs further strengthening the halocline and reducing any mixing/dispersion of the low $\delta^{18}O$ waters into the sub-surface layers, a positive feedback mechanism is established that continues until meltwater input ceases. Under this chain of events, considerable less meltwater input is required to generate the observed changes in SSS than would be expected at other open ocean sites around the globe.

Additional short-term changes in meltwater input to the region may have been further enhanced by the opening/closure of the Bering Sea Straits. Whilst Pliocene changes remain unconstrained, (Matthiessen et al., 2009), sea-level fluctuations of 40-80 m (Miller et al., 2005) suggest the status of the Bering Straits gateway may have undergone several changes over both long, glacial-interglacial, and shorter, millennial, timescales between MIS G6 and MIS 99. An open gateway would typically be expected to increase flow through the Bering Straits and into the North Atlantic Ocean (Marincovich and Gladenkov, 1999). Depending on the timing of the straits closure, increased export of fresher water from the North Pacific/Bering Sea into the North Atlantic Ocean during the initial, c. 4 psu, SSS decline at 2.73 Ma and subsequent interglacial/glacial transitions could have assisted in the permanent glaciation of Greenland by lowering SST and SSS in the East Greenland Current and reducing Meridional Overturning Circulation (MOC) (Sarnthein et al., 2009). Alone these changes would not significantly alter the SSS or $\delta^{18}O_{water}$ at ODP Site 882. However in an open gateway state, models have demonstrated that the direction of Arctic throughflow can reverse following a MOC shut down, increasing the input of isotopically light water to the Bering Sea and so North Pacific Ocean via flow across the Aleutian Island Arc and Kamchatka Straits (De Boer and Nof, 2004a,b; Hu and Meehl, 2005; Hu et al., 2007). Similarly in a closed state the reduced export of freshwater from the North Pacific/Bering Sea to the North Atlantic can increase MOC (Hu et al., 2010), potentially increasing glacier melting around the North Pacific/Bering Sea Basin and so further lower SSS at ODP Site 882. Whilst both these processes are short-lived, ranging from years to decades for reversed Arctic flow (De Boer and Nof, 2004b) and centennial to millennial timescales for increased MOC/glacial melting (Hu et al., 2010), and so insufficient to explain the long-term glacial-interglacial changes in SSS at ODP Site 882, these processes may be important for understanding the abrupt short-term SSS variations that are apparent during both interglacial and glacial eras (Fig. 4b).

Although much of this discussion remains circumstantial and whilst the relationship between changes in $\delta^{18}O_{diatom}$ and glacial/interglacial state remains poorly constrained, invoking a glacial meltwater mechanism combined with possible additional inputs arising from changes in the Bering Straits gateway remains at this time the most pragmatic explanation for the observed changes in $\delta^{18}O_{diatom}$. Given the above assumptions in calculating changes in SSS and the lack of consideration for mixing processes which would have further altered the SSS:$\delta^{18}O$ end-member during the transportation of fresh/meltwater to ODP Site 882, the reconstructed values should not be regarded as absolute indication of SSS change. In addition, given that calculated changes in $\delta^{18}O_{water}$ and SSS are closely driven by $\delta^{18}O_{diatom}$ with only negligible contributions from changes in SST (Haug et al., 2005) and global ice volume (Lisiecki and Raymo, 2005), it is necessary for these findings to be replicated at other sites including those in the Bering Sea.

4.2 Halocline water column

Repeated shift of $\delta^{18}O_{diatom}$ during the interglacials of MIS G3, G1, 103 and 101 to values in excess of +42‰, equivalent to those in the interval prior to the onset of major NHG at 2.73 Ma would typically be expected to coincide with alterations between a mixed (interglacial)/stratified (glacial) water column if rates of decreased/increased meltwater input were sufficient to overturn/trigger the halocline. This would be analogous to the initial transition from a mixed to stratified water column at 2.73 Ma which has been associated with a significant increase in freshwater input to the region (Sigman et al., 2004; Haug et al., 2005; Swann et al., 2006; Nie et al., 2008). Three lines of evidence, however, suggest that an uninterrupted halocline prevailed over the analysed interval.

Firstly, a switch to a mixed water column would be expected to culminate in the upwelling of cold as well as nutrient rich deep water to the surface, instigating increases in opal MAR and decreases in SST. Relatively low opal MAR of 0-1.2 g/cm^2/ka and warm SST of >10ºC, except in MIS 103 and the end of MIS 101, therefore suggest that there was no reversal to a mixed, high productivity, system similar to that which prevailed prior to 2.73 Ma (Haug et al., 1999; 2005) (Fig. 3). Given that diatom growth in the modern North Pacific Ocean is constrained by iron limitation (e.g., Harrison et al., 1999; Tsuda et al., 2003; Yuan and Zhang, 2006), it is plausible that similar mechanisms prevailed from MIS G5 onwards to prevent any increase in opal concentrations in a mixed water column state. At open sites such as ODP Site 882 situated away from continental influences, Fe availability is primarily controlled by aeolian deposition (Duce and Tindale, 1991; Jickells et al., 2005) which in the North West Pacific Ocean predominantly originates from the Badain Juran Desert, China (Yuan and Zhang, 2006). Records at other sites in the North Pacific over the last 200 ka BP have documented changes in aeolian fluxes aligned with accumulation rates at the Chinese Loess Plateau (Kawahata et al., 2000). If changes in Chinese Loess MAR are similarly used over the interval from 2.73 Ma to 2.52 Ma as a tracer of aeolian and so iron flux to ODP Site 882, the influence of iron availability on biological productivity can be discounted with no relationship between changes in loess accumulation and opal MAR (Fig. 3). Accordingly, the absence of any significant rise in opal concentrations can be attributed to the change in SSS being insufficient to remove the halocline stratification rather than the presence of an iron limited mixed water column.

A second line of evidence to suggest a permanent halocline originates from comparisons of the $\delta^{18}O_{diatom}$ and planktonic $\delta^{18}O_{foram}$ data from ODP Site 882. Modern day *C. marginatus* and *C. radiatus* diatom frustules in the region primarily bloom during autumn/early winter (Takahashi, 1986; Takahashi et al., 1996; Onodera et al., 2005). As such, in a stratified state, changes in the input of isotopically light/heavy waters would have affected conditions in the uppermost part of the surface ocean at depths extending down to the seasonal late summer-early winter thermocline at 50 m and potentially to the halocline at c. 100-150 m (Andreev et al., 2002; Antonov et al 2006; Locarnini et al., 2006). Although planktonic $\delta^{18}O_{foram}$ records are of insufficient resolution to provide further information as to the origin of the isotopically light/heavy water (Fig. 3) (Maslin et al., 1996, 1998), it is notable that *Globigerina bulloides* and *Neogloboquadrina pachyderma* are often found at much lower depths within the surface ocean including at depths below the modern day halocline (Kohfield et al., 1996; Kuroyanagi and Kawahata, 2004). The absence of any marked alteration in the low resolution planktonic $\delta^{18}O_{foram}$ after 2.73 Ma, compared to $\delta^{18}O_{diatom}$, therefore imply that water inputs were restricted to the uppermost parts of the photic zone and did not extend into deeper sections of the surface ocean as would be expected in a mixed water column scenario (Fig. 3). Due to the extreme scarcity of preserved foraminifera in the sediment record, additional planktonic $\delta^{18}O_{foram}$ measurements can not be made to further assess issues regarding the vertical penetration of any freshwater inputs.

Final, quantitative, evidence for a permanent halocline can be found be calculating the change in SSS required to initiate an overturning of the stratification. Modern day waters above the halocline (c. 100-150 m) around ODP Site 882 are marked by year round potential densities (σ_θ for $\rho = 0$) of <26.8 kg/m^3 (c.f., Fofonoff and Millard 1983; Antonov et al., 2005; Locarnini et al., 2005). By assuming that a density of 26.8 kg/m^3 is also applicable for the halocline boundary in the Pliocene/early Quaternary and using a coccolith U^k_{37} SST record from ODP Site 882 (Haug et al., 2005), the SSS required to obtain a potential density >26.8 kg/m^3 and so water column overturning can be back calculated using seawater equations of state (Fofonoff and Millard 1983). With regional fluxes of coccoliths similar to the analysed diatom taxa in being focused towards autumn/early winter (Ohkouchi et al., 1999; Harada et al., 2006; Seki et al., 2007), results will be representative of the months when overturning would be expected to occur. Results, however, show that the necessary SSS required to remove the halocline and generate deep water mixing, i.e., to increase the photic zone potential density to >26.8 kg/m^3, is never reached except at 2.65 Ma (Fig. 4b). In particular, calculations show that where SSS is greater than that in the mixed water column prior to 2.73 Ma, e.g., at the onset of MIS G3, the higher SST that accompany these intervals are sufficient to counter-act these rises by lowering the potential density of the photic zone and so increase the salinity threshold needed to generate overturning. Changing the potential density of the halocline boundary used in these calculations from 24.8 kg/m^3 to 27.8 kg/m^3 alters the SSS threshold required for overturning by only 0.00-0.09 psu. Therefore it can be concluded that whilst significant, the reduced freshwater inputs to ODP Site 882 during interglacials from MIS G5 to MIS 99 were insufficient to increase SSS to the levels required to generate deep water mixing.

With regards to why no evidence exists for a short-lived transition to a mixed water column at 2.65 Ma when SSS are greater than the modelled SSS threshold required for overturning, one possibility is that the net decrease in rates of freshwater influx to the region were not enough on a seasonal/annual timeframe to raise SSS beyond the necessary threshold. Additional consideration must also be given to the accuracy of the SSS:$\delta^{18}O$ end-member used in the SSS reconstruction and the potential for the true end-member to be outside the range used in Section 4.1. Whilst the possible range and temporal variability of SSS:$\delta^{18}O$ end-members for the North Pacific Basin are unknown over this interval, existing research has demonstrated that the $\delta^{18}O$ values of individual ice-sheets vary considerably in Eurasia and North America at the Last Glacial Maximum with values of −16‰ to −40‰ and −28‰ to −34‰ respectively (Duplessy et al., 2002). Further work is therefore required involving the use of regional ice-sheet/ocean circulation models to fully investigate the nature and origin of increased freshwater input to the North West Pacific Ocean and the exact magnitude of change in SSS.

5 Conclusions

In spite of large changes in $\delta^{18}O_{diatom}$ indicating significant variations in freshwater influx to the subarctic North West Pacific Ocean over the late Pliocene/early Quaternary, no evidence exists to suggest that the halocline stratification boundary was ever removed. Such findings concur with evidence of low opal MAR from 2.73 Ma onwards which indicate a transition to a stratified system and the region shifting from a major net source to a minor net sink of CO_2 potentially similar to the modern day (Haug et al., 1999; Honda et al., 2002; Chierici et al., 2006). Given the magnitude of change in $\delta^{18}O_{water}$ required to cause the observed shifts in $\delta^{18}O_{diatom}$ and SSS, further research is needed through oceanic and climate models to assess the origin of the freshwater inputs to the region and to determine the extent to which these inputs may have altered nutrient fluxes to the photic zone and so the biological pump. The most logical origin for increased freshwater input, given the magnitude of $\delta^{18}O_{diatom}$ changes, is for a glacial meltwater source. Although little is known about the extent and size of glaciers around the North Pacific basin, attributing the changes in $\delta^{18}O_{diatom}$ to primarily originate from such a source would imply that regional glaciers were well developed in the late Pliocene following the intensification of major Northern Hemisphere Glaciation. Understanding such issues are increasingly important given the potential role of the Pliocene in providing an analogue for investigating future climate scenarios under a warmer climate (Jansen et al., 2007; Haywood et al., 2009).

Acknowledgements

This research was funded by a NERC postdoctoral fellowship award to GEAS (NE/F012969/1). Thanks are owed to Sam Jaccard for proving the high resolution opal MAR data from 2.78-2.61 Ma BP, Michael Sarnthein for discussions on the $\delta^{18}O_{diatom}$ dataset and two anonymous reviewers for their constructive comments on the manuscript.

References

Andreev, A., Kusakabe, M., Honda, M., Murata, A., Saito C., 2002. Vertical fluxes of nutrients and carbon through the halocline in the western subarctic Gyre calculated by mass balance . Deep-Sea Research II 49, 5577-5593.

Antonov, J.I., Locarnini, R.A., Boyer, T.P., Mishonov, A.V., Garcia, H.E., 2006. Volume 2: Salinity, in: Levitus, S. (Ed.), World Ocean Atlas 2005, NOAA Atlas NESDIS 62, U.S. Government Printing Office, Washington, D.C., pp. 182.

Bailey, I, Bolton, C.T., DeConto, R.M., Pollard, D., Schiebel, R., Wilson, P.A., 2010. A low threshold for North Atlantic ice-rafting from 'low slung slippery' late Pleistocene ice-sheets. Paleoceanography PA1212, doi:10.1029/2009PA001736.

Bigg, G,R., Clark, C.D., Hughes, A.L.C., 2008. A last glacial ice sheet on the Pacific Russian coast and catastrophic change arising from coupled ice–volcanic interaction. Earth and Planetary Science Letters 265, 559-570.

Brandriss, M.E., O'Neil, J. R., Edlund, M.B., Stoermer, E.F., 1998. Oxygen isotope fractionation between diatomaceous silica and water. Geochimica et Cosmochimica Acta, 62 1119-1125.

Chierici, M., Fransson, A., Nojiri, Y., 2006. Biogeochemical processes as drivers of surface fCO_2 in contrasting provinces in the subarctic North Pacific Ocean. Global Biogeochemical Cycle 20, GB1009, doi: 10.1029/2004GB002356.

Clayton, R.N., Mayeda T.K., 1963. The use of bromine pentafluoride in the extraction of oxygen from oxide and silicates for isotope analysis. Geochimica et Cosmochimica Acta 27, 43–52.

De Boer, A.M., Nof, D., 2004a. The exhaust valve of the North Pacific. Journal of Climate 17, 417-422.

De Boer, A.M., Nof, D., 2004b. The Bering Strait's grip on Northern Hemisphere climate. Deep Sea Research I 51, 1347-1366.

Deino, A.L., Kingston, J.D., Glen, J.M., Edgar, R.K., Hill, A., 2006. Precessional forcing of lacustrine sedimentation in the late Cenozoic Chemeron Basin, Central Kenya Rift, and calibration of the Gauss/Matuyama boundary. Earth and Planetary Science Letters 247, 41-60.

Duce, R.A., Tindale, N.W., 1991. Atmospheric transport of iron and its deposition in the ocean. Limnology and Oceanography 36, 1715-1726.

Duplessy, J.D., Bard, E., Labeyrie, L., Dupart, J., Moyes, J., 1993. Oxygen-isotope records and salinity changes in the Northeastern Atlantic Ocean during the last 18,000 years. Paleoceanography 8, 341-350.

Duplessy, J-C., Labeyrie, L., Waelbroeck, C., 2002. Constraints on the oxygen isotopic enrichment between the Last Glacial Maximum and the Holocene: Paleoceanographic implications. Quaternary Science Reviews 21, 315-330.

Fofonoff, P., Millard R.C., 1983. Algorithms for computation of fundamental properties of seawater. Unesco Technical Papers in Marine Science, 44, 53 pp.

Gebhardt, H., Sarnthein, M., Grootes, P.M., Kiefer, T., Kuehn, H., Schmieder, F., Rohl, U., 2008. Paleonutrient and productivity records from the subarctic North Pacific for Pleistocene glacial terminations I to V. Paleoceanography 23, PA4212, doi:10.1029/2007PA001513.

Harada, N., Sato, M., Shiraishi, A., Honda, M.C., 2006. Characteristics of alkenone distributions in suspended and sinking particles in the northwestern North Pacific. Geochimica et Cosmochimica Acta 70, 2045-2062.

Harrison, P.J., Boyd, P.W., Varela, D.E., Takeda, S., Shiomoto, A., Odate, T., 1999. Comparison of factors controlling phytoplankton productivity in the NE and NW subarctic Pacific gyres. Progress in Oceanography 43, 205-234.

Haug, G.H., Sigman, D.M., Tiedemann, R., Pedersen, T.F., Sarnthein, M., 1999. Onset of permanent stratification in the subarctic Pacific Ocean. Nature 401, 779-782.

Haug, G.H., Ganopolski, A., Sigman, D. M., Rosell-Mele, A., Swann, G.E.A., Tiedemann, R., Jaccard, S, Bollmann, J., Maslin, M.A., Leng, M.J., Eglinton, G., 2005. North Pacific seasonality and the glaciation of North America 2.7 million years ago. Nature 433: 821-825.

Haywood, A.M., Dowsett, H.J., Valdes, P.J. Lunt, D.J., Francis, J.E., Sellwood, B.W., 2009. Introduction. Pliocene climate, processes and problems. Philosophical Transactions of the Royal Society A 367, 3-17.

Hillebrand, H., Dürselen, C-D., Kirschtel, D., Pollingher, U., Zohary, T., 1999. Biovolume calculation for pelagic and benthic microalgae. Journal of Phycology 35, 403-424.

Honda, M.C., Imai, K., Nojiri, Y., Hoshi, F., Sugawarad, T., Kusakabe, M., 2002. The biological pump in the northwestern North Pacific based on fluxes and major components of particulate matter obtained by sediment-trap experiments (1997–2000). Deep-Sea Research II 49, 5595–5625.

Hu, A., Meehl, G.A., 2005. Bering Strait throughflow and the thermohaline circulation. Geophysical Research Letters 32, L24610, doi:10.1029/2005GL024424.

Hu, A., Meehl, G.A., Han, W., 2007. Role of Bering Strait in the thermohaline circulation and abrupt climate change. Geophysical Research Letters, 34, L05704, doi:10.1029/2006GL028906.

Hu, A., Meehl, G.A., Otto-Bliesner, L., Waelbroeck, C., Han, W., Loutre, M-F., Lambeck, K., Mitrovica, J.X., Rosenbloom, N., 2010, Influence of Bering Strait flow and North Atlantic circulation on glacial sea-level changes. Nature Geosciences 3, 118-121.

IODP Expedition 323., Scientists, 2010. Bering Sea paleoceanography: Pliocene-Pleistocene paleoceanography and climate history of the Bering Sea. IODP Preliminary Report 323, doi:10.2204/iodp.pr.323.2010.

Jansen, E., Overpeck, J., Briffa, K.R., Duplessy, J-C., Joos, F., Masson-Delmotte,m V., Olago, D., Otto-Bliesner, B., Peltier., W.R., Rahmstorf, S., Ramesh, R., Raynaud, D., Rind, D., Solomina, O., Villalba, R., Zhang, D., 2007. Palaeoclimate, in Solomon, S., Qin, D., Manning, M., Chen, Z., Marquis, M., Averyt, K.B., Tignor, M., Miller, H.L., (Eds.), Climate Change 2007: The physical science basis. Contribution of Working Group I to the Fourth Assessment Report of the Interngovernmental Panel on Climate Change. Cambridge University Press, Cambridge, UK.

Jickells, T.D., An, Z.S., Andersen, K.K., Baker, A.R., Bergametti, G., Brooks, N., Cao, J.J., Boyd, P.W., Duce, R.A., Hunter, K.A., Kawahata, H., Kubilay, N., laRoche, J., Liss, P.S., Mahowald, N., Prospero, J.M., Ridgwell, A.J., Tegen, I., Torres, R., 2005. Global iron connections between desert dust, ocean biogeochemistry, and climate. Science 308, 67-71.

Kawahata, H., Okamoto, T., Matsumoto, E., Ujiie, H., 2000. Fluctuations of eolian flux and ocean productivity in the mid-latitude North Pacific during the last 200 kyr. Quaternary Science Reviews 19, 1279-1292.

Kohfeld, K.E., Fairbanks, R.G., Smith, S.L., Walsh, I.D. 1996. *Neogloboquadrina pachyderma* (sinistral coiling) as paleoceanographic tracers in polar oceans: evidence from Northeast Water Polynya plankton tows, sediment traps, and surface sediments. Paleoceanography 11, 679-699.

Kotilainen, A.T., Shackleton, N.J. 1995. Rapid climate variability in the North Pacific Ocean during the past 95,000 years. Nature 377, 323-326.

Krissek, L.A., 1995. Late Cenozoic ice-rafting records from Leg 145 Sites in the North Pacific: Late Miocene onset, Late Pliocene intensification, and Pliocene-Pleistocene events. In Rea, D.K., Basov, I.A., Scholl, D.W., Allan, J. F., (Eds.), *Proc. ODP, Scientific Results*, 145, College Station, Texas, pp. 283-292.

Kuroyanagi, A., Kawahata, H., 2004. Vertical distribution of living planktonic foraminifera in the seas around Japan. Marine Micropaleontology 53, 173-196.

LeGrande, A.N., Schmidt, G.A., 2006. Global gridded data set of the oxygen isotopic composition in seawater. Geophysical Reearch Letters 33, L12604, doi:10.1029/2006GL026011.

Lehmann, M., Siegenthaler, U., 1991. Equilibrium oxygen- and hydrogen- isotope fractionation between ice and water. Journal of Glaciology 37, 23-26.

Leng, M.J., Sloane, H.J., 2008. Combined oxygen and silicon isotope analysis of biogenic silica. Journal of Quaternary Science 23, 313-319.

Lisiecki, L.E., Raymo M.E., 2005. A Pliocene-Plesitocene stack of 57 globally distributed benthic $\delta^{18}O$ records. Paleoceanography 20, PA1003: doi:10.1029/2004PA001071.

Locarnini, R.A., Mishonov, A.V., Antonov, J.I., Boyer, T.P., Garcia, H.E., 2006. Volume 1: Temperature, in Levitus, S., (Ed.), World Ocean Atlas 2005, NOAA Atlas NESDIS 61, U.S. Government Printing Office, Washington, D.C., pp. 182.

Macdonald, R.W., Paton, D.W., Carmack, E.C., Omstedt, A., 1995. The freshwater budget and under-ice spreading of Mackenzie River water in the Canadian Beaufort Sea based on salinity and $^{18}O/^{16}O$ measurements in water and ice. Journal of Geophysical Research 100 (C1), 895-919.

Majoube, M., 1971. Fractionnement en oxygen et en deuterium entre l'eau et sa vapeur. Journal de Chimie et de Physique 68, 1423.

Marincovich, L. Jr., Gladenkov, A.Y., 1999. Evidence for an early opening of the Bering Straits.Nature 397, 149-151.

Maslin, M.A., Haug, G.H., Sarnthein, M., Tiedemann, R., 1996. The progressive intensification of northern hemisphere glaciation as seen from the North Pacific. Geologische Rundschau 85, 452-465.

Maslin, M.A., Shackleton, N.J., Pflaumann, U., 1995. Surface water temperature, salinity, and density changes in the northeast Atlantic during the last 45,000 years: Heinrich events, deep water formation, and climatic rebounds. Paleoceanography 10, 527-544.

Matthiessen, J., Knies, J., Vogt, C., Stein, R., 2009. Pliocene palaeoceanography of the Arctic Ocean and subarctic seas. Philosophical Transactions of the Royal Society A 367, 21-48.

McKelvey, B.C., Chen, W., Arculus, R.J., 1995. Provenance of Pliocene-Pleistocene ice rafted debris, Leg 145, Northern Pacific Ocean, in Rea D.K., Basov I.A., Scholl D.W., and Allan J.F., (Eds.), *Proc. ODP, Scientific Results*, 145, College Station, Texas, pp. 195-204.

Morley, D.W., Leng, M.J., Mackay, A.W., Sloane, H.J., Rioual, P., Battarbee, R.W., 2004. Cleaning of lake sediment samples for diatom oxygen isotope analysis. Journal of Paleolimnology 31, 391-401.

Moschen, R., Lücke, A., Schleser, G., 2005. Sensitivity of biogenic silica oxygen isotopes to changes in surface water temperature and palaeoclimatology. Geophysical Research Letters 32, L07708, doi:10.1029/2004GL022167.

Nie, J., King, J., Liu, Z., Clemens, S., Prell, W., Fang, X., 2008. Surface-water freshening: a cause for the onset of North Pacific stratification from 2.75 Ma onward? Global and Planetary Change 64, 49-52.

Ohkouchi, N., Kawamura, K., Kawahata, H., Okada, H., 1999. Depth ranges of alkenone production in the central Pacific Ocean. Global Biogeochemical Cycles 13, 695-704 .

Onodera, J., Takahashi, K. 2005. Silicoflagellate fluxes and environmental variations in the northwestern North Pacific during December 1997–May 2000. Deep Sea Research I 52, 371-388.

Reynolds, B.C., Frank, M., Halliday, A.N., 2008. Evidence for a major change in silicon cycling in the subarctic North Pacific at 2.73 Ma. Paleoceanography 23, PA4219, doi:10.1029/2007PA001563.

Sarnthein, M., Bartoli, G., Prange, M., Schmittner, A., Schneider., B., Weinelt, M., Andersen, N.,Garbe-Schönberg, D., 2009. Mid-Pliocene shifts in ocean overturning circulation and the onset of Quaternary-style climates. Climates of the Past 5, 269-283.

Seidov, D., Maslin, M., 1999. North Atlantic deep water circulation collapse during Heinrich events. Geology 27, 23-26.

Schlitzer, R., 2009. Ocean Data View, http://odv.awi.de.

Seki, O. Nakatsuka, T., Kawamura, K., Saitoh, S-I., Wakatsuchi, M., 2007. Time-series sediment trap record of alkenones from the western Sea of Okhotsk. Marine Chemistry104, 253-265.

Sigman, D.M., Jaccard, S.L., Haug, G.H., 2004. Polar ocean stratification in a cold climate. Nature 428, 59-63.

St John, K.E.K., Krissek, L.A., 1999. Regional patterns of Pleistocene ice-rafted debris flux in the North Pacific. Paleoceanography 14, 653-662.

Sun, Y., An, Z., 2005. Late Pliocene-Pleistocene changes in mass accumulation rates of eolian deposits on the central Chinese Loess Plateau. Journal of Geophysical Research 110, D23101, doi:10.1029/2005JD006064.

Sun, Y., Clemens, S.C., An, Z., Yu, Z., 2006. Astronomical timescale and palaeoclimatic implication of stacked 3.6-Myr monsoon records from the Chinese Loess Plateau. Quaternary Science Reviews, 25, 33-48.

Swann, G.E.A., Maslin, M.A., Leng, M.J., Sloane, H.J., Haug, G.H., 2006. Diatom δ^{18}O evidence for the development of the modern halocline system in the subarctic northwest Pacific at the onset of major Northern Hemisphere glaciation. Paleoceanography 21, PA1009, doi: 10.1029/2005PA001147.

Swann, G.E.A., Leng, M.J., Sloane, H.J., Maslin, M.A., Onodera, J., 2007. Diatom oxygen isotopes: evidence of a species effect in the sediment record. Geochemistry, Geophysics, Geosystems 8, Q06012, doi:10.1029/2006GC001535.

Swann, G.E.A., Leng, M.J., Sloane, H.J., Maslin, M.A., 2008. Isotope offsets in marine diatom δ^{18}O over the last 200 ka. Journal of Quaternary Science 23, 389-400.

Swann, G.E.A., Leng, M.J., 2009. A review of diatom δ^{18}O in palaeoceanography. Quaternary Science Reviews 28, 384-398.

Takahashi, K., 1986. Seasonal fluxes of pelagic diatoms in the subarctic Pacific, 1982-1983. Deep-Sea Research 33, 1225-1251.

Takahashi, K., Hisamichi, K., Yanada, M., Maita, Y., 1996. Seasonal changes of marine phytoplankton productivity: a sediment trap study. Kaiyo Monthly 10, 109-115. [In Japanese]

Tian, J., Wang, P., Cheng, X., 2004. Development of the East Asian monsoon and Northern Hemisphere glaciation: oxygen isotope records from the South China Sea. Quaternary Science Reviews 23, 2007-2016.

Tian, J., Pak, D.K., Wang, P., Lea, D., Cheng, X., Zhao, Q., 2006. Late Pliocene monsoon linkages in the South China Sea. Earth and Planetary Science Letters 252, 72-81.

Tiedemann, R., Haug, G. H., 1995. Astronomical calibration of cycle stratigraphy for Site 882 in the northwest Pacific, in Rea D.K., Basov I.A., Scholl D.W., and Allan J.F., (Eds.), *Proc. ODP, Scientific Results*, 145, College Station, Texas, pp. 283-292.

Tsuda, A., Takeda, S., Saito, H., Nishioka, J., Nojiri, Y., Kudo, I., Kiyosawa, H., Shiomoto, A., Imai, K., Ono, T., Shimamoto, A., Tsumune, D., Yoshimura, T., Aono, T., Hinuma, A., Kinugasa, M., Suzuki, K., Sohrin, Y., Noiri, Y., Tani, H., Deguchi, Y., Tsurushima, N., Ogawa, H., Fukami, K., Kuma, K., Saino, T., 2003. A Mesoscale Iron Enrichment in the Western Subarctic Pacific Induces a Large Centric Diatom Bloom. Science 300: 958-961.

Yuan, W., Zhang, J., 2006. High correlations between Asian dust events and biological productivity in the western North Pacific. Geophyisical Research Letters 33: L07603, doi:10.1029/2005GL025174.

Zhang, Y.G., Ji, J., Balsam, W., Liu, L., Chen, J., 2009. Mid-Pliocene Asian monsoon intensification and the onset of Northern Hemisphere glaciation. Geology 37, 599-602.

Supplementary Data

Supplementary Table 1: $\delta^{18}O_{diatom}$ data used within this study with the relative species biovolume composition of the samples.

Figure captions

Figure 1: Location of ODP Site 882 (50°22'N, 167°36'E) in the North West Subarctic Pacific Ocean. Map created using Ocean Data View version 4.1.3 (Schlitzer et al., 2009).

Figure 2: Relative diatom species biovolumes in purified samples analysed for $\delta^{18}O_{diatom}$.

Figure 3: Changes in $\delta^{18}O_{diatom}$ within the 75-150 μm fraction alongside existing ODP Site 882 records of magnetic susceptibility as a proxy for IRD (Haug et al., 1999), U^{k}_{37} SST (Haug et al., 2005), opal MAR (Haug et al., 1999; Sigman et al., 2004) and planktonic $\delta^{18}O_{foram}$ (Maslin et al., 1996, 1998) in addition to a global stacked benthic $\delta^{18}O_{foram}$ record (Lisiecki and Raymo, 2005), a Chinese Loess Plateau magnetic susceptibility (Sun et al., 2006) and Hm/Gt ratios from the South China Sea (Zhang et al., 2009). $\delta^{18}O_{diatom}$ data is a combination of samples analysed within this study (circles) and data published in Swann et al. (2006) (triangles). ODP Site 882 magnetic susceptibility records displays both the raw data (grey) and a loess curve (black). Chinese Loess Plateau magnetic susceptibility and Hm/Gt ratios used as proxy of monsoon activity/precipitation. For planktonic $\delta^{18}O_{foram}$, black (triangles) and blue (circles) records represents *G. bulloides* and *N. pachyderma* (dextral) respectively. Following Reynolds et al. (2008) the age of the stacked benthic $\delta^{18}O_{foram}$ record has been adjusted by +10 ka to position the Matuyama/Gauss boundary at 2.61 Ma on the orbital time scale (Deino et al., 2006). Shaded regions after the development of the halocline at 2.73 Ma indicates periods of high $\delta^{18}O_{diatom}$ values equivalent to those in the pre-2.73 Ma interval of mixed water column conditions.

Figure 4: A) Changes in surface water $\delta^{18}O_{water}$ at ODP Site 882 calculated from $\delta^{18}O_{diatom}$ by accounting for changes in SST using a U^{k}_{37} SST record (Haug et al., 2005) with a diatom-temperature coefficient of 0.2‰/°C (Brandriss et al., 1998; Moschen et al., 2005) and using a global stacked benthic $\delta^{18}O_{foram}$ record (Lisiecki and Raymo, 2005) to correct for variations in global ice volume. Fluxes of both the coccolith derived alkenones and analysed diatoms are focused towards autumn/early winter (Takahashi, 1986; Takahashi et al., 1996; Ohkouchi et al., 1999; Onodera et al., 2005; Harada et al., 2006; Seki et al., 2007). B) Changes in salinity calculated using SSS:$\delta^{18}O$ end-member ratios of 1-0.5 (polygon) together with the modelled SSS threshold required to overturn the halocline boundary by increasing the potential density of the

photic zone to >26.8 kg/m^3 (dashed line). Shaded regions after the development of the halocline at 2.73 Ma indicates periods of high $\delta^{18}O_{diatom}$/$\delta^{18}O_{water}$/SSS values equivalent to those in the pre-2.73 Ma interval of mixed water column conditions.

Figure 1

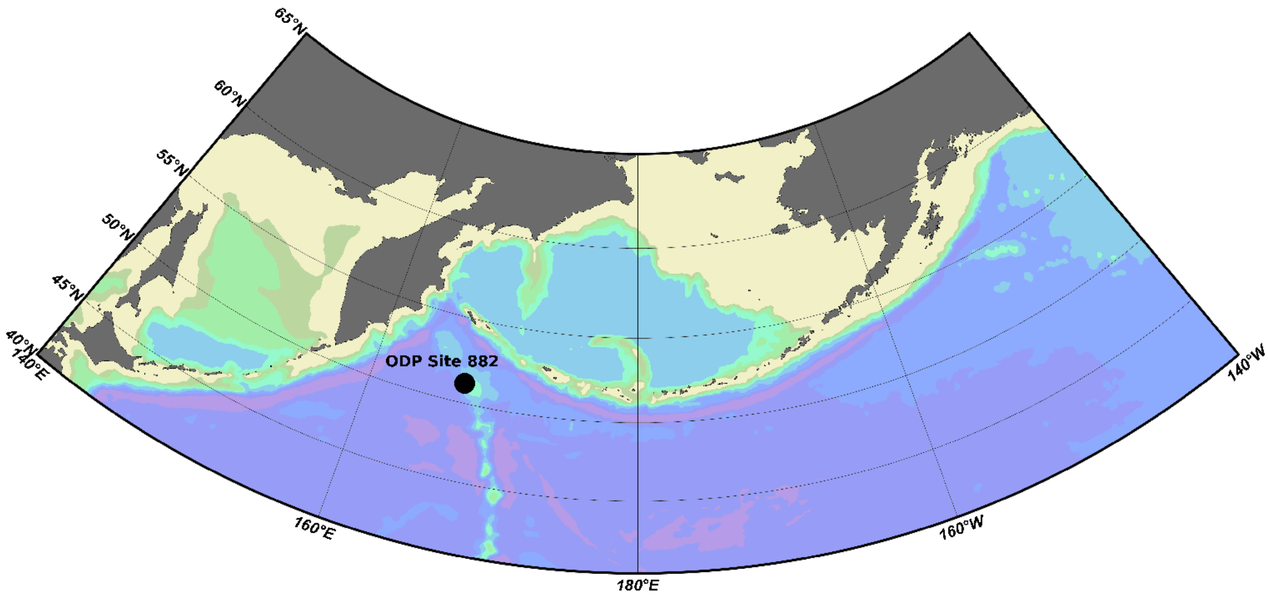

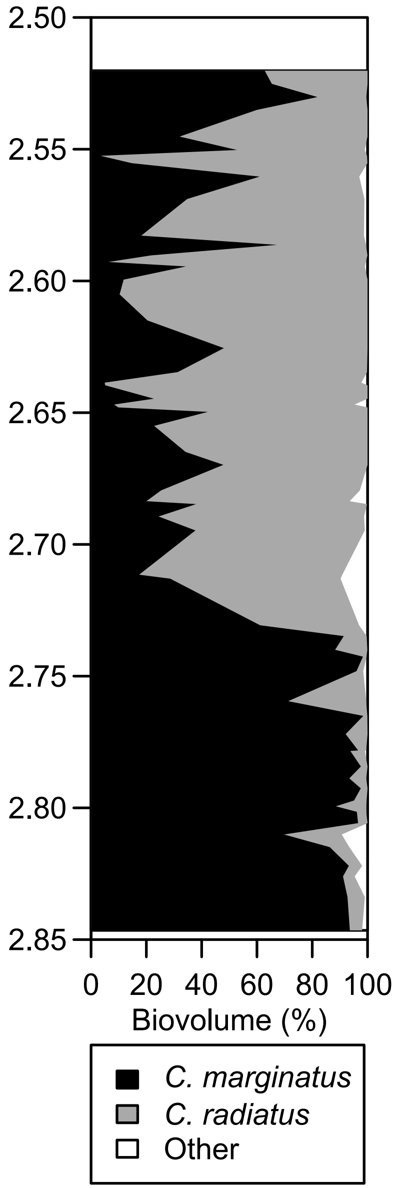
2.50
2.55
2.60
2.65
2.70
2.75
2.80
2.85
0
20
40
60
80
100
Biovolume (%)
C. marginatus
C. radiatus
Other

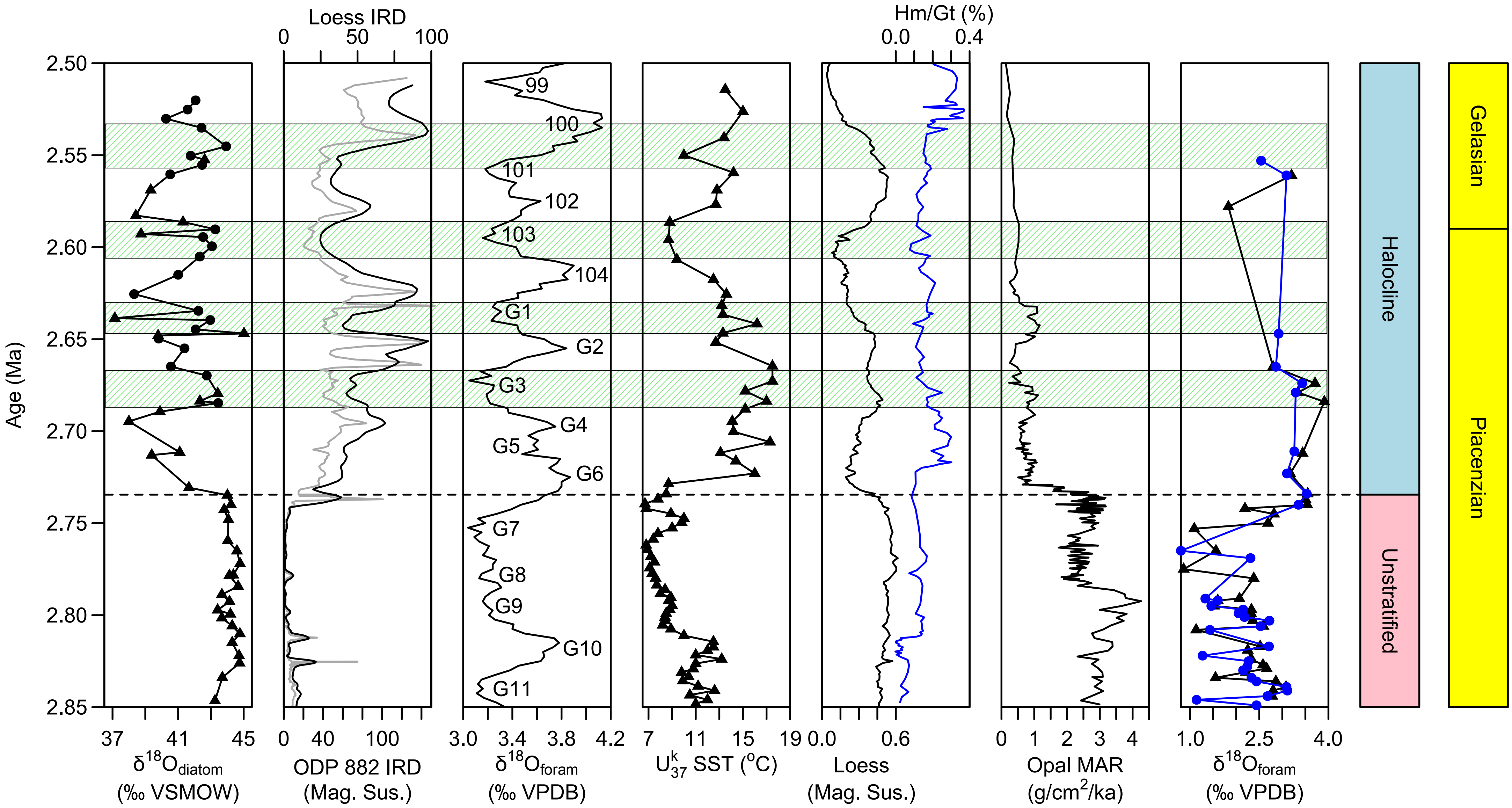

Age (Ma)
δ18Odiatom (‰ VSMOW)
Loess IRD
ODP 882 IRD (Mag. Sus.)
δ18Oforam (‰ VPDB)
99
100
101
102
103
104
G1
G2
G3
G4
G5
G6
G7
G8
G9
G10
G11
Uk37 SST (oC)
Hm/Gt (%)
Loess (Mag. Sus.)
Opal MAR (g/cm2/ka)
δ18Oforam (‰ VPDB)
Halocline
Unstratified
Gelasian
Piacenzian

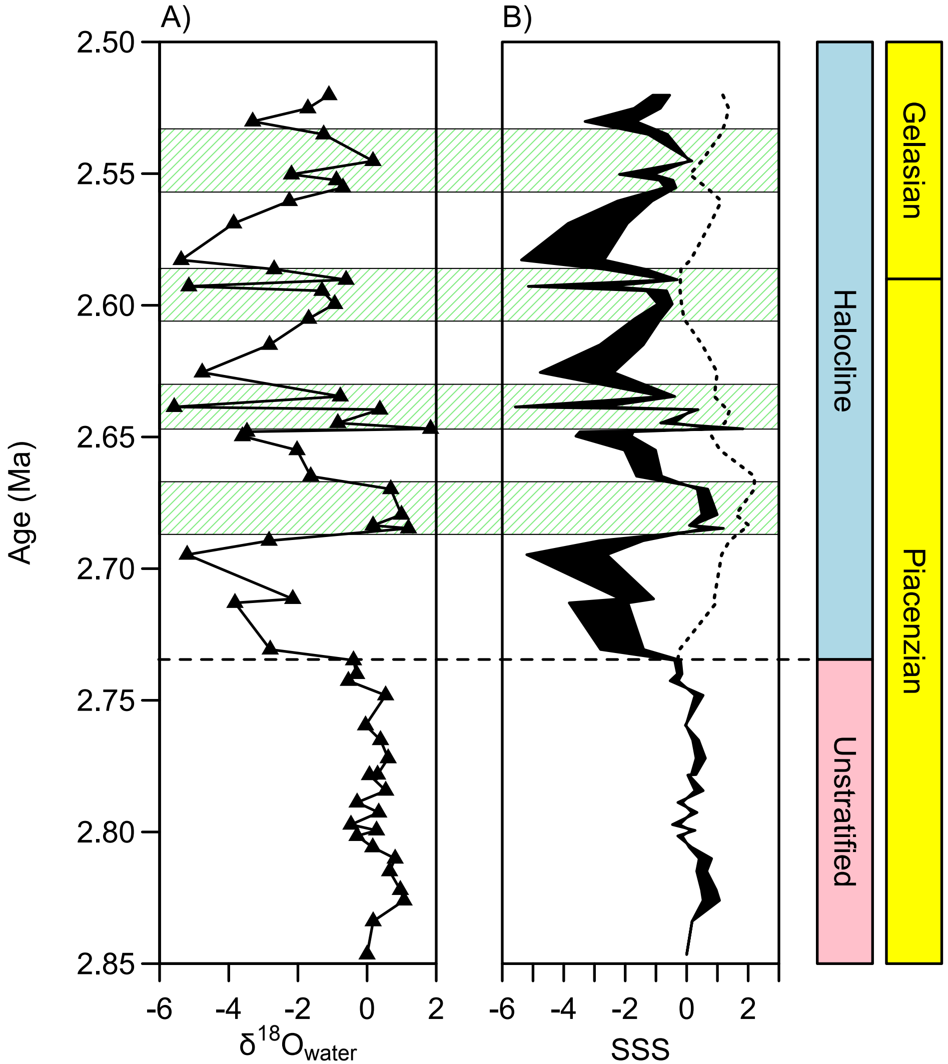
A)
B)
Age (Ma)
2.50
2.55
2.60
2.65
2.70
2.75
2.80
2.85
-6
-4
-2
0
2
$\delta^{18}O_{water}$
SSS
Halocline
Unstratified
Gelasian
Piacenzian